River Flow 2010 - Dittrich, Koll, Aberle & Geisenhainer (eds) - © 2010 Bundesanstalt für Wasserbau ISBN 978-3-939230-00-7

Unsteady flow in a channel with large scale bank roughness

T. Meile
HydroCosmos SA, Grand-Rue 43, 1904 Vernayaz, Switzerland

J.-L. Boillat & A. J. Schleiss
Laboratory of Hydraulic Constructions (LCH), Ecole Polytechnique Fédérale de Lausanne (EPFL), Station 18, 1015 Lausanne, Switzerland

ABSTRACT: Systematic investigations on positive and negative surge waves from upstream have been conducted in a 40 m long channel with a mean bed slope of 1.14‰ and non-prismatic bank geometries. The channel banks included macro-roughness elements, namely various cavities. In total, 41 different geometrical configurations have been investigated. The surge wave experiments confirmed the applicability of the elementary surge wave theory including secondary waves and wave breaking in the prismatic reference configuration. In geometries with channel bank macro-roughness, the absolute surge wave celerity V_w and the celerity surge wave celerity c are reduced. Among other reasons, the observed reduction of the absolute surge wave celerity is due to the increased flow resistance and lays between 5% and 30% for both, positive and negative waves from upstream. Due to the dispersive character, the positive and negative surges from upstream are characterized by a sudden change (front), followed by a progressive change (body) of the water level. Under the influence of bottom slope and friction, the height of the front of a surge wave is reduced exponentially along the channel. This reduction can be described by a simple mathematical model. Its calibration on the surge wave experiments pointed out the extra diffusion due to the macro-scale roughness.

Keywords: Unsteady flow, Macro-roughness, Surge wave experiments

1 INTRODUCTION

Many anthropogenic actions and natural events, namely sluice gate operations, flushing of reservoirs, debris jam and break up, ice jam and break up, sudden stopping and starting of turbines of runoff river and storage hydropower plants, flash-floods etc. can lead to rapidly varied unsteady flow in open channels. High-head storage hydropower plants for example mainly operate their turbines during periods of high energy demand. Even if under the influence of bottom slope and friction, surges often do not appear, the sudden starting and stopping of turbines, called hydropeaking, might cause rapidly varied unsteady flow in smooth channels with small slopes. Morphological measures such as lateral cavities at the banks can increase the flow resistance and the natural retention capacity of rivers. Thus, depending entities such as the propagation speed or the height of the surge wave front are modified in complex geometries with large scale or macro-roughness.

Experiments with highly unsteady flow in the field of open channel hydraulics mainly cover three domains: First, experiments of dam break waves due to a sudden failure of a dam (e.g. Schoklitsch 1917; Dressler 1954; Lauber and Hager 1998a, 1998b; Leal et al. 2006, Boillat et al. 2008), secondly experiments dealing with positive and negative surge waves from upstream or downstream due to sluice gate or fast turbine operations including a baseflow (e. g. Favre 1935) and finally experiments focusing on secondary waves. These waves are also called “Favre waves” and occur behind the wave front (Favre 1935, Faure and Nahas 1961; Benet and Cunge 1971; Zairov and Listrovoy 1983; Treske 1994; Soares and Zech 2002).

First systematic investigations on the propagation speed of small positive and negative surge waves from upstream and downstream in a channel have been presented by Bazin (1865). The important theoretical and experimental work of Favre (1935) resulted in equations for the determination of the absolute wave celerity and the height of the surge wave front due to a sudden change in dis-

charge. Further experiments with surge waves including a downstream base flow have been done by Ünsal (1983), Zairov and Listrovoy (1983).
This paper presents the results of systematic surge wave experiments with positive and negative surges from upstream in geometries characterized by large scale or macro-roughness at the channel banks. The experiments include a steady flow downstream of the surge wave front and have been conducted under controlled laboratory conditions. The main goal of the study is to highlight the influence of large scale depression roughness, increasing the flow resistance and natural retention capacity, on surge wave propagation and deformation.

2 THEORETICAL BACKGROUND

The unsteady, non-uniform and rapidly varied flow is characterized by a free surface having sudden change and high curvature. As a consequence, assumption of hydrostatic pressure might not be valid on a limited channel reach. A sudden change of the discharge or water-level can cause a rapidly varied flow called surge wave. Namely four different types of surge waves are defined (Favre 1935, Chow 1959, Henderson 1966, Graf and Altinakar 1996): the positive surge wave moving downstream, the positive surge wave moving upstream, the negative (surge) wave moving downstream and the negative (surge) wave moving upstream.

In a horizontal, rectangular channel of width B without friction, having a baseflow $Q_1 = U_1 \cdot B \cdot h_1$, an increase of the discharge at the upstream channel border always leads to a positive surge with a steep front. The water-surface discontinuity, called a positive surge from upstream, travels downstream with an absolute celerity V_w of the surge wave front:

$$V_w = U_1 + \sqrt{g h_1} \cdot \sqrt{\frac{h_2}{2h_1}\left(1+\frac{h_2}{h_1}\right)} \qquad (1)$$

The negative surge from upstream, the positive surge from downstream and the negative surge from downstream are defined analogously (e.g. Henderson 1966). If the disturbance compared to the baseflow depth is small, (1) becomes:

$$V_w = U_1 + \sqrt{g h_1} \qquad (2)$$

Neither the height of the surge wave front h' nor the propagation speed are modified along the frictionless, horizontal and rectangular channel (Figure 1, above). In natural channels or rivers, where the channel slope and friction have to be considered, the propagation of a surge depends on dynamic processes caused by the inclination of the water-surface. Favre (1935) proposes an explicit calculation method for surge waves which are superimposed to a uniform or gradually varied steady or unsteady baseflow in prismatic configurations including friction and slope. The proposed method is based on a small ratio of h'/h_1 and also applies to channels having different cross-sections.

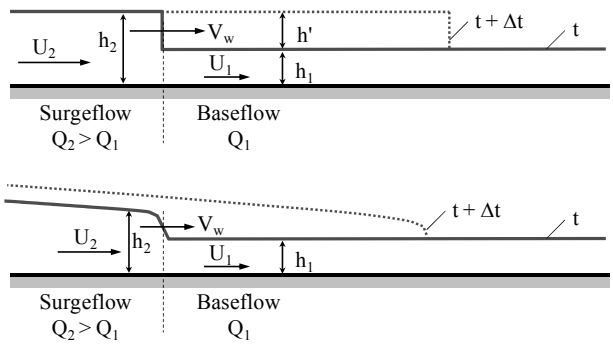

Figure 1: Positive surge from upstream in the horizontal, prismatic and frictionless channel (above) and in the channel including bottom and friction slope (below). U = mean flow velocity, h = flow depth, h' = surge height, Q = discharge, t = time. The indices *1* and *2* refer to the pre- and post-surge conditions.

When friction and bottom slope are taken into account (Figure 1, below), the height of the surge wave front exponentially decreases along the channel and the wave body deforms (Favre 1935; Zairov and Listrovoy 1983). Furthermore, a positive surge having a steep front does not necessarily develop by the increase of the discharge at the upstream end of the channel under the influence of friction and bottom slope. Based on, first the applicability of the Chezy formula for describing the flow resistance, secondly the assumption of a wide channel of constant bottom slope and third the assumption of a relatively small disturbance, Henderson (1966) developed a criteria relative to the surge formation of a positive wave:

$$\frac{dh}{dt} \geq \frac{g h_0 S_0 \left(2 - Fr_0\right)\left(1 + Fr_0\right)}{3U_0} \qquad (3)$$

where h is the flow depth, t the time, h_0 the normal flow depth, S_0 the constant bottom slope, Fr_0 the Froude number and U_0 the mean flow velocity corresponding to the normal flow depth. The right side term of this equation is negative if $Fr_0 > 2$. This means that for every positive disturbance dh/dt, the condition for the formation of a surge is satisfied. For $Fr_0 < 2$, the rate of change of the flow depth must exceed a minimum value in order to be higher than the right side term. Due to the three assumptions, the applicability of (3) is however rather limited and in many practical cases, the question concerning the surge formation is solved more efficiently by numerical methods

based on the de Saint-Venant equations. Furthermore, the numerical schemes solving the depth averaged de Saint-Venant equations have been found working well for many practical applications (Hicks et al. 1991).

3 EXPERIMENTS

3.1 *Flume and geometrical configurations*

The test flume has a useful length of 38.33 m and a mean slope of 1.14 ‰ (Figure 2). It is divided from upstream to downstream into an inlet reach (length 7.41 m), a reach with large scale depressions at the banks (26.92 m) and an outlet reach (4.0 m). The sidewalls of the reach with rectangular cavities and the outlet reach are formed by smooth limestone bricks.

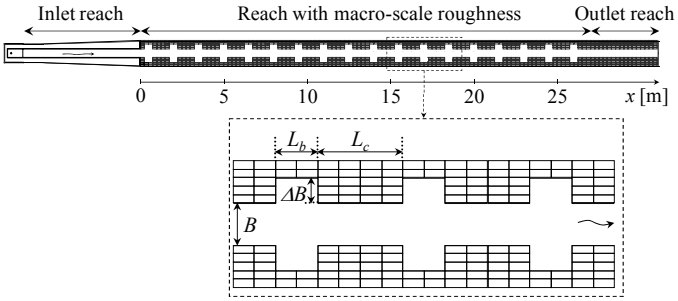

Figure 2: Situation of the test flume. Variable parameters of the macro-rough configurations are L_b, L_c and ΔB.

The channel base width is $B = 0.485 \pm 0.002$ m and remained constant during all the tests. The macro-roughness elements considered in this research are large scale depression roughness (Morris 1955) at both channel banks. Three geometrical parameters namely the length of the cavity L_b, the distance between two cavities L_c and the lateral extent of the cavities ΔB, are systematically varied (Figure 2). Table 1 summarizes the range of the investigated geometrical parameters L_b, L_c and ΔB as well as derived ratios.

The aspect and expansion ratios of the cavity are defined as $AR = \Delta B / L_b$ and $ER = (B + 2\Delta B) / B$ respectively. The combination of three different values for L_b and L_c and four different values of ΔB results in the 36 different, axi-symmetric geometrical configurations covering 8 aspect and 4 expansion ratios. Additionally, three of the 36 axi-symmetric configurations have been tested in an asymmetric arrangement and a randomly generated configuration has also been analyzed.

The equivalent sand roughness of the limestone bricks without macro-roughness has been determined by means of backwater curve computations in the rectangular, prismatic reference configuration. Friction coefficients have been calculated using the logarithmic law with the constants of Rouse (1965). The equivalent sand roughness of the wall and the bottom are k_{sw}=0.021 mm and k_{s0}=0.001 mm respectively. The channel bed made of smooth painted steel is fix without sediment transport. The discharge is introduced at the upstream border of the channel through a 0.5 m wide and 0.9 m long, horizontal opening of the inlet basin. At the downstream border of the channel, the flow depth is controlled by a particularly shaped cross section (Carlier 1972). It corresponds almost to the normal flow depth of the prismatic channel without macro-roughness.

Table 1. Summary of test range of geometrical parameters

Cavity length L_b	0.5 m, 1.0 m, 2.0 m
Distance between cavities L_c	0.5 m, 1.0 m, 2.0 m
Lateral extent of the cavity ΔB	0.1 m, 0.2 m, 0.3 m, 0.4 m
Aspect ratios $\Delta B / L_b$	0.05, 0.10, 0.15, 0.20, 0.30, 0.40, 0.60, 0.80
Expansion ratios $(B+2\Delta B) / B$	1.41, 1.82, 2.24, 2.65

3.2 *Steady flow tests*

The aim of the first test phase on steady flow was to determine the flow resistance of the macro-rough configurations (Meile 2007; Meile et al. 2008a, Meile et al. 2008b) by means of backwater-curve computations and by minimizing the last square errors (Sieben 2003). Flow conditions have been investigated for up to 12 different steady discharges between $0.0037 < Q < 0.1255$ m^{3}s^{-1} for each geometrical configuration. The discharge during the tests was controlled by an electromagnetic flow meter. Characteristic values of Froude $Fr = U \cdot (g \cdot h)^{-1}$ and Reynolds $Re = U \cdot R_h \cdot \nu^{-1}$ number relative to the base width B ranged between $0.37 < Fr < 0.64$ and $6'800 < Re < 110'000$ for typical flow depths between 0.03 m $< h <$ 0.34 m and mean flow velocities between $0.24 < U < 0.80$ ms^{-1}. The water levels have been recorded with ultrasonic sensors located along the channel axis.

3.3 *Unsteady flow tests*

The aim of the phase of the unsteady flow tests was to evaluate the influence of the macro-roughness on the propagation, attenuation and deformation of positive and negative surge waves from upstream. The investigated surge waves have been superimposed to a steady baseflow.

A selected amount of discharge can be added rapidly to the well established baseflow to generate the surge waves. To do this, an upper basin with an individual water supply system has been placed on the flume over the inlet basin of the channel. The upper and the inlet basin were connected by four

pipes of different diameters. The sudden opening or closure of one or several pipe(s) causes the positive or negative surges from upstream. Every geometrical configuration has been investigated under 5 to 30 scenarios of rapidly varied unsteady flow (Table 2).Positive surges include additional flows that present 9 % to 900 % of the baseflow. Negative surges include sudden flow reduction which amounts for 9 % to 90 % of the baseflow. Scenarios 3, 8, 13, 18, and 23 (Table 2) have been systematically tested for every configuration. All other scenarios have been investigated for geometrical configurations with ΔB=0.2 m and ΔB=0.4 m only.

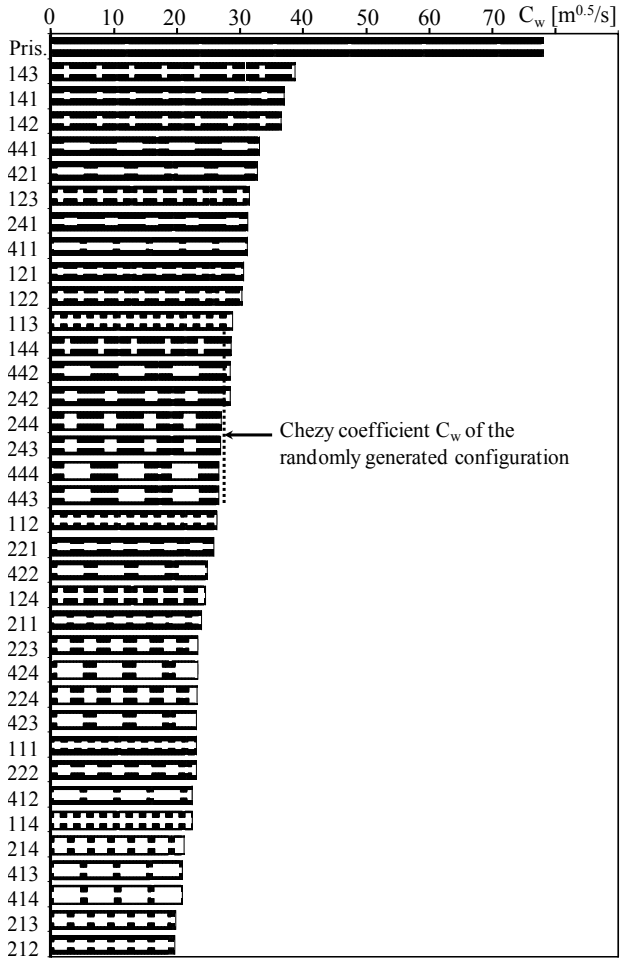

Figure 3: Typical Chezy coefficients C_w of the macro-rough configurations relative to the wall (relative flow depth $h/B \cong 0.6$ to 0.7) for 37 tested configurations.

Table 2. Unsteady flow tests: scenarios 1 to 30. The total discharge Q_{total} at the channel inlet after complete opening and stabilization of the flow is given in the brackets in [l/s].

Operated flaps	Baseflow before positive surge [litres/s]					
[-]	≈6	≈11	≈19	≈35	≈49	≈63
Pipe 1	1 (12.5)	6 (17.3)	11 (25.9)	16 (41.4)	21 (55.4)	26 (69.3)
Pipe 2	2 (17.2)	7 (21.9)	12 (30.5)	17 (46.0)	22 (59.9)	27 (73.8)
Pipe 1 & 2	**3** (23.6)	**8** (28.4)	**13** (36.9)	**18** (52.3)	**23** (66.2)	28 (80.1)
Pipe 1 & 3	4 (36.5)	9 (41.1)	14 (49.7)	19 (65.0)	24 (78.8)	29 (92.6)
Pipe 1, 2 & 4	5 (59.6)	10 (64.2)	15 (72.5)	20 (87.7)	25 (101.3)	30 (115.0)

The propagation of the surge waves along the flume has been recorded by the ultrasonic level sensors regularly spaced along the channel. In the prismatic configuration, velocity measurements have been performed additionally using an Ultrasonic Velocity Profiler (Meile et al. 2008c).

4 RESULTS

4.1 *Highly unsteady flow in prismatic and macro-rough configurations*

According to the wave classification criteria of Ponce et al. (1978) and Chung and Kang (2006), all the positive waves from upstream of scenarios 3, 8, 13, 18 and 23 (Table 2) are classified in the domain of gravity waves after the formation in the inlet reach. The investigated negative waves are mainly gravity waves at the origin, but they rapidly transform into dynamic waves due to their dispersive character along the channel.

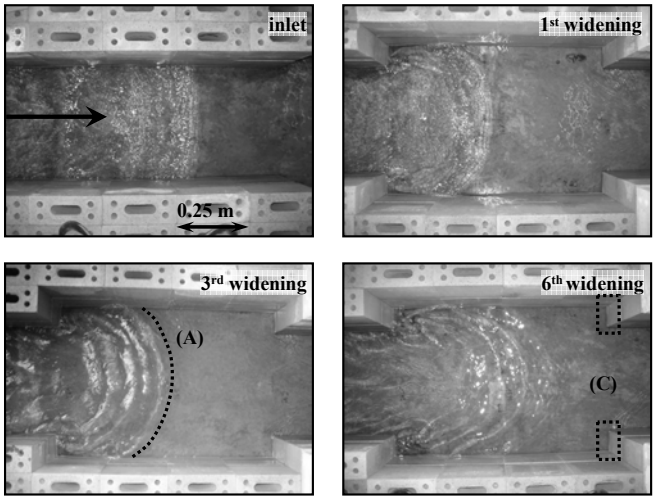

Figure 4: Positive surge wave from upstream: L_b = 1.0 m; L_c = 0.5 m, ΔB = 0.1 m. Q_{base} = 6.38 l/s; Q_{total} = 24.93 l/s. (A) Deformation and (C) reflection of surge wave.

However, the propagation of the positive and negative surge waves along the macro-rough reach revealed some major differences between the prismatic reference configuration and the various macro-rough configurations. The absolute surge wave celerity is reduced in the macro-rough configurations (§ 4.2) and the attenuation rate of the height of the surge wave front is increased (§ 4.3). In the prismatic channel the elementary surge wave theory relative to the propagation speed and the attenuation of the height of the surge wave front is confirmed. In the macro-rough configurations the surge wave front deforms and becomes three dimensional, especially in the cavities of the widened channel reaches (Figure 4).

The detection of the exact position of the wave front is more difficult in the macro-rough configurations due to a weak and heterogeneous water-surface. In the prismatic reference configuration,

the water surface is quite homogeneous before and after the surge front which makes easier the detection of the surge front.

At the wave front, different conditions have been observed for both, prismatic and macro-rough configurations: 1) breaking surge wave front 2) breaking of the first undulation of the surge wave followed by secondary waves, also called "Favre waves" 3) non breaking surge wave front followed by secondary waves 4) non breaking surge wave front without detectable secondary undulations.

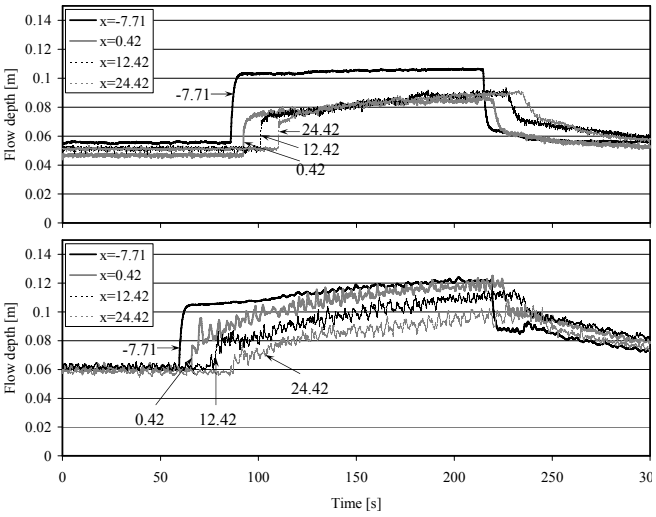

Figure 5: Example of a positive surge followed by a negative surge. Above: in the prismatic channel. Below: in the macro-rough channel, L_b = 1 m, L_c = 1 m, ΔB = 0.2 m. $Q_{base} \cong$ 11 l/s, $Q_{total} \cong$ 28 l/s in both experiments.

The investigations in the prismatic configuration confirmed the formation of Favre waves after and before the surge front for ratios of the flow depth higher than $h_2 / h_1 > 1.1$. The height of Favre waves increases until the ratio reaches $h_2 / h_1 \cong 1.42$ for which the first undulation is breaking. For higher values, the relative height of secondary waves decreases rapidly and they disappear completely for a value of $h_2 / h_1 \cong 1.6$. For this and higher values, the surge wave front is characterized by highly breaking flow conditions and a significant, local air entrainment. The relative spacing e / h' of the wave crests decreases as a function of the relative surge wave height (Figure 6). For the prismatic reference configuration, the observed spacing between the first and second crest is stabilized at ultrasonic sensor 13 since no major difference can be observed compared to ultrasonic sensor 21 further downstream. At ultrasonic sensor 5, the distance between the first two wave crests is not established yet especially for relative surge wave heights $h' / h_1 < 0.25$. The relative spacing of well established secondary waves observed in the laboratory flume of the present study is given by:

$$\frac{e}{h'} = 4.5\left(\frac{h'}{h_1}\right)^{-5/4}, (R^2 = 0.98) \quad (4)$$

Considering also the data of Favre (1935) equation (4) becomes:

$$\frac{e}{h'} = 4.5\left(\frac{h'}{h_1}\right)^{-7/5}, (R^2 = 0.98) \quad (5)$$

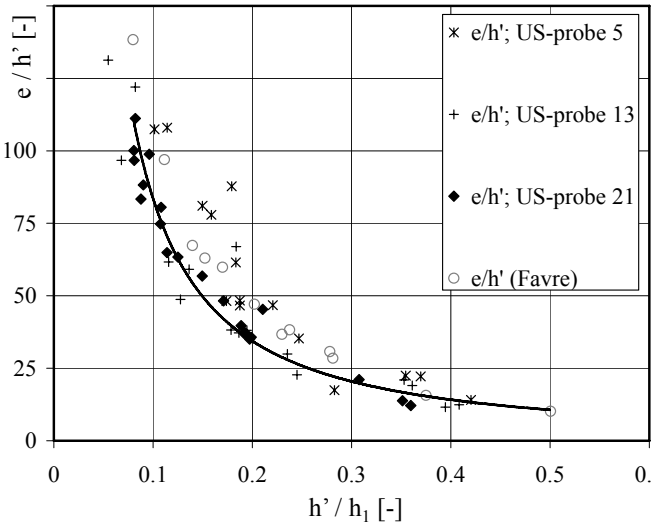

Figure 6: Relative spacing e / h' of the wave crests. Ultrasonic sensor 5, 13 and 21 are located at the channel sections x_5 = 0.42 m, x_{13} = 12.42 m and x_{21} = 24.42 m (Figure 2).

In the macro-rough configurations, the conditions at the surge wave front are modified when the wave travels downstream. For example, surge waves having a breaking front in the prismatic configuration might become surge waves with a non breaking front followed by secondary waves in some macro-rough configurations. Surge waves with a non breaking front followed by secondary waves might transform into a non breaking surge without secondary waves etc.

Further insight into the characteristics of the flow around a breaking surge wave front is obtained from the unsteady velocity profiles measured in the prismatic configuration. For this type of surge waves, a "two-layer" velocity profile has been detected during the short period corresponding to the passage of the front. A faster part moving on a lower, slower part is observed during a very short period which equals a short distance in the surge wave body (Meile et al. 2008c). Hence, for the investigated, breaking conditions of the surge wave front, significantly non hydrostatic pressure distributions (due to an accelerated velocity profile) are limited to a very small wave part. This physically explains the disappearance of the secondary waves (Soares and Zech 2002) in case of breaking conditions.

4.2 *Surge wave front speed*

The absolute wave celerities along the macro-rough reach have been found practically constant, but reduced when compared to the prismatic reference. The reduction of $V_w^+ = U + c^+$ lays between 5% (configurations 141, 241 and 441) and 25% (configurations 114, 214 and 414) compared to the prismatic reference where U is a representative mean flow velocity of the baseflow and c^+ the wave celerity of a positive surge. The decrease of V_w^- ranges approximately around 15% compared to the prismatic reference (25% for 114 to 5% for 441). The reduction is exemplarily shown for 5 of the 41 investigated macro-rough configurations as a function of the observed upstream surge Froude number Fr_s (Figure 7).

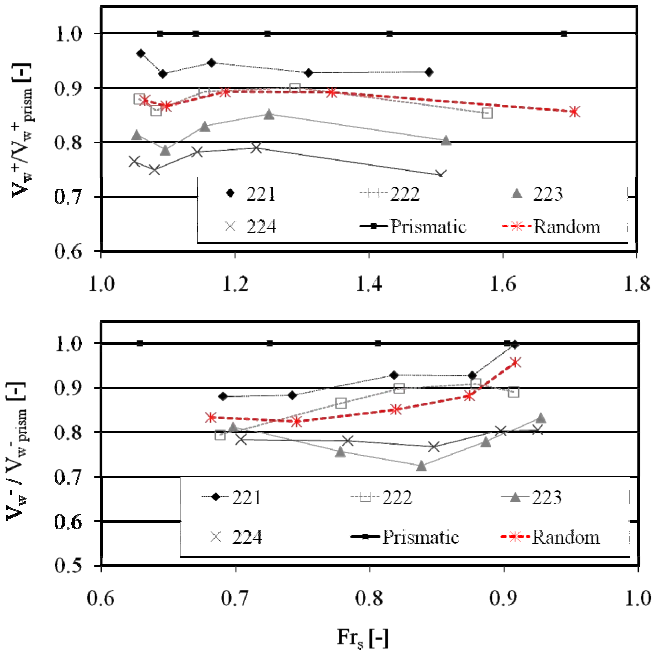

Figure 7: Relative reduction of the absolute surge wave celerity of the positive and negative surge waves from upstream. The experiments have all L_b = 1 m, L_c = 1 m, whereas ΔB varies between 0.1 m (221) and 0.4 m (224).

$$Fr_s = \frac{(V_w - U_1)}{\sqrt{gh_1}} = \sqrt{\frac{h_2}{2h_1^2}(h_2 + h_1)} \qquad (6)$$

Further analysis has been done on the relative celerities c^+ and c^-, by correcting V_w^+ and V_w^- with a representative mean flow velocity U_1^+ corresponding to the conditions before the positive surge respectively U_1^- before the negative surge.

$$U_1^+ = \frac{\sum_i x_i \cdot Q_{base} / B_{eff} \cdot h_i}{x_{total}} \qquad (7)$$

$$U_1^- = \frac{\sum_i x_i \cdot Q_{total} / B_{eff} \cdot h_i}{x_{total}} \qquad (8)$$

x_i = length for which h_i (flow depth measured at sensor i) is representative. x_{total} is the sum of all x_i. B_{eff} is equal to the base width of the channel (for the prismatic configuration and for the parts between cavities) or computed taking into account an expansion of the flow into the macro scale depression roughness elements as:

$$B_{eff} = (B + \Delta B)\left(\frac{x\Delta B}{L_b}\right) + (B + 2\Delta B)\left(\frac{L_b - x\Delta B}{L_b}\right) \qquad (9)$$

where x describes the expansion of the flow (Meile 2007):

$$x = \left(\frac{\mathrm{Re}_{\lim}}{\mathrm{Re}_m} + x_0\right)\left(\frac{L_b}{\Delta B}\right)^{0.18} \qquad (10)$$

with Re_{lim} = 150'000 and x_0 = 4.5, found from the experiments under steady flow conditions.

The comparisons between the observed celerities ($c = V_w - U$) and the calculated, ones (from the measured flow depths before and after the surge front, Eq. (1)) are shown in Figure 8 and 9. For some geometrical configurations, the observed macro-rough positive and negative celerities are close to the calculated ones. However, for most scenarios and configurations, the observed celerities are significantly reduced, namely between 5% and 20% for the positive and between 0% and 20% for the negative surge waves from upstream.

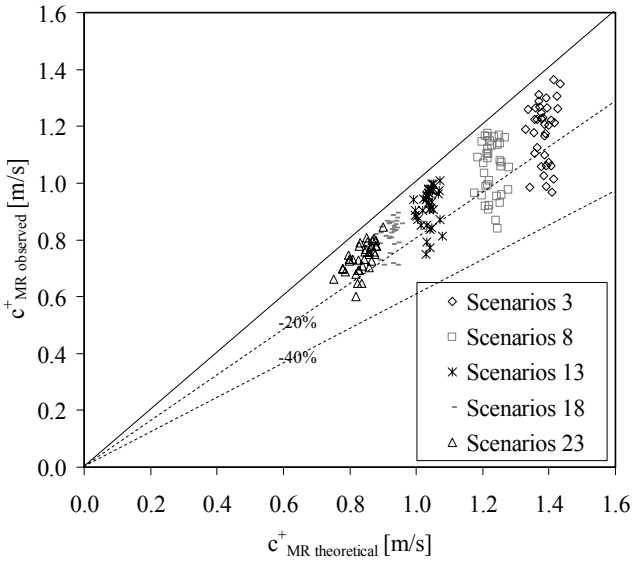

Figure 8: Positive surge wave celerities after subtraction of a representative mean flow velocity U_1^+ (Eq. 7, 9 and 10).

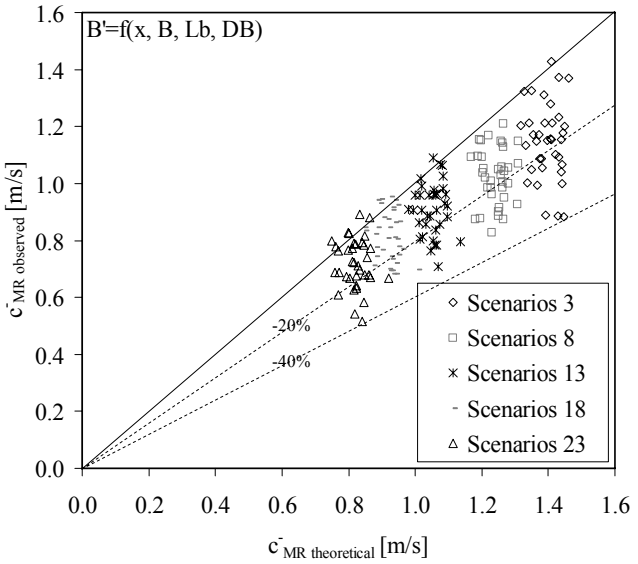

Figure 9: Negative surge wave celerities after subtraction of a representative mean flow velocity U_1^- (Eq. 8, 9 and 10).

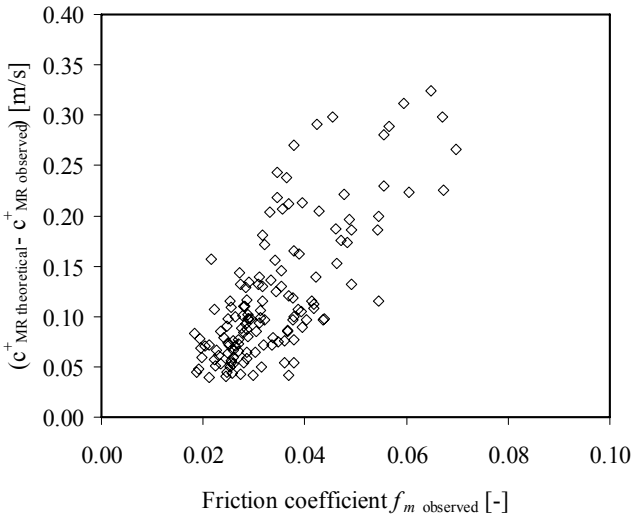

Figure 10: Difference between $c_{MR\ theoretical}$ and $c_{MR\ observed}$ as a function of the friction coefficient. The friction coefficient relates to Q_b and is obtained from the steady flow tests.

The difference between the theoretical celerities in the horizontal channel $c_{MR\ theoretical}$ and the observed celerities $c_{MR\ observed}$ for the positive surge waves correlates with the identified friction coefficient $f_m = f_{prism} + f_{MR}$ under steady flow conditions.

Figure 10 supports the assumption that the decrease of the celerities in the macro-rough configurations depends at least partially on the flow resistance similar to the observed decrease of the front celerity of a dam break wave under the influence of friction (Dressler 1954, Whitham 1955, a and Hager 1998a 1998b, Leal et al. 2006).

4.3 *Attenuation of the surge wave front height*

The analysis of the surge wave front height confirms the dispersive character of surge waves. The extra dispersion in the macro-rough configurations varies and is the result of the macro-rough flow resistance and other phenomena such as the partial reflections of the surge wave in the cavities of the macro-roughness elements and the passive retention in the cavities.

Along the prismatic channel, the ratio between the surge wave height upstream and downstream of the experimental channel h'^{+}_{ds}/h'^{+}_{us} indicates a decrease of the surge wave front height of 5% (for low ratios Q_{total}/Q_b) to 25% (for high Q_{total}/Q_b). In the macro-rough configurations, the decrease is significantly higher (up to 70%). The height of the negative surge front $(h'^{-}_{ds} / h'^{-}_{us})$ decreases along the prismatic channel of 5% to 25%. The decrease of h'^{-} ranges between 10% and 75% along the channel with macro-roughness at the banks.

The attenuation of the surge wave front height can be described with the following equation which is adapted from Lai et al. (2000):

$$\frac{h'(x)}{h'(x_0)} = e^{(-(\boldsymbol{a}+\boldsymbol{b})\cdot X)} \qquad (11)$$

where $h'(x)$ = wave front height at a distance x of the channel, $h'(x_0)$ = initial wave front height at the reference location x_0. The dimensionless distance X takes into account the channel slope S_0 (a priori constant) and the depth of the baseflow h_b (a priori uniform and steady):

$$X = \frac{x - x_0}{(h_b / S_0)} \qquad (12)$$

The attenuation parameters of the wave front height in the prismatic channel are $\boldsymbol{a}^+ = 0.39$ for the positive surge wave and $\boldsymbol{a}^- = 0.99$ for the negative surge wave. The additional attenuation of the surge wave front height due to macro-roughness and storage of water inside the cavities can be described with the parameter $\boldsymbol{b}$.

The values of $\boldsymbol{b}$ have been determined for all experiments with different macro-rough configurations by fitting the theoretical curve of Eq. (11) to the observed values $h'(x)/h'(x_0)$. With this data set and by using the technique of the **E**volutionary **P**olynomial **R**egression method (Giustolisi and Savic 2006), the parameters $\boldsymbol{b}^+$ and $\boldsymbol{b}^-$ are:

$$\boldsymbol{b}^+ = 26.5 \cdot \left(\frac{L_b + L_c}{\Delta B}\right) \cdot f_{MR} \cdot \ln\left(\frac{2\Delta B L_b}{B(L_b + L_c)} + 1\right)$$

$(R^2 = 0.77)$ (13)

$$\boldsymbol{b}^- = 1.47 \cdot \left(\frac{2\Delta B L_b}{B(L_b + L_c)}\right) \cdot \ln\left(\frac{L_b + L_c}{\Delta B} + 1\right) + 37.7 \cdot f_{MR}$$

$(R^2 = 0.71)$ (14)

The attenuation parameter depends on geometrical parameters of the macro-rough configurations as well as on the macro-rough friction coefficient

f_{MR} corresponding to the situation before the passing of the surges from upstream

The uniform baseflow depth conditions are verified in the present experimental study only for the prismatic reference, which limits the range of application for quantitative results to comparable situations, namely bottom slopes close to 0.001 and backwater-curves of the type M2. However, comparative results might be extended to other cases.

5 CONCLUSIONS

Systematic experiments of positive and negative surge waves have been conducted in prismatic and macro-rough channels. For the prismatic reference configuration the elementary surge wave theory and the developments of Favre (1935) are confirmed. Due to the curvature of the wave front (positive surge), leading to extra pressure terms, secondary waves can be observed for wave height ratios between $1.1 < h_2 / h_1 < 1.6$. The spacing of wave crests can be estimated by using equation (5). For higher ratios, secondary waves disappear.

The absolute wave celerities along the macro-rough reach have been found practically constant, but reduced when compared to the prismatic reference. The reduction of V_w^+ lays between 5% and 25% compared to the prismatic reference. The decrease of V_w^- ranges approximately around 15% compared to the prismatic reference. Among other reasons (backwater-curve effects, the partial expansion of the flow in the widened channel reaches and the reduction of the surge wave height), the reduction of the absolute surge wave celerities in the macro-rough configurations is due to the increased flow resistance.

The dispersive character of surge waves is experimentally observed. The front height decreases in particular in the macro-rough configurations. The attenuation of the surge wave front height can be described with the empirical formula (11) including a dimensionless distance X (12) and the attenuation parameters $\boldsymbol{a}$ and $\boldsymbol{b}$ ((13) for $\boldsymbol{b}^+$ and for (14) $\boldsymbol{b}^-$), which refer to the prismatic and macro rough attenuation respectively.

REFERENCES

Bazin, H. 1865. Recherches expérimentales relatives aux remous et à la propagation des ondes. Dunod, Paris, 528-553.

Benet, F., Cunge, J. A. 1971. Analysis of Experiments on Secondary Undulations caused by Surge Waves in Trapezoidal Channels. Journal of Hydraulic Research - IAHR, 9(1), 11-33.

Boillat, J.-L., Ribeiro, J., Duarte, A., Darbre, G. 2008. Dambreak in case of silted up reservoirs. Proc. of River Flow 2008, Ed. Altinakar, M.S. et al., Izmir-Cesme, Turkey, 6-8 Sept. 2008, 903-909.

Carlier, M. 1972. Hydraulique générale et appliquée, Eyrolles, Paris, France.

Chow, V. T. 1959. Open-channel hydraulics, McGraw-Hill New York, USA.

Chung, W., Kang, Y. 2006. Classifying River Waves by the Saint Venant Equations Decoupled in the Laplacian Frequency Domain. Journal of Hydraulic Engineering - ASCE, 132(7), 666-680.

Dressler, R. F. 1954. Comparison of theories and experiments for the hydraulic dambreak wave. International Association of Scientific Hydrology, 3(38), 319-328.

Faure, J., Nahas, N. 1961. Etude numérique et expérimental d'intumescences à forte courbure du front. Intumescences - Société hydrotechnique de France, 5, 579-587.

Favre, H. 1935. Etude théorique et expérimentale des ondes de translation dans les canaux découverts, Dunod, Paris.

Giustolisi, O., Savic, D. A. 2006. A Symbolic Data-driven Technique Based on Evolutionary Polynomial Regression. Journal of Hydroinformatics, 8(3), 207–222.

Graf, W. H., Altinakar, M. S. 1996. Hydraulique fluviale, écoulement non permanent et phénomènes de transport. PPUR, Lausanne, Switzerland.

Henderson, F. M. 1966. Open Channel Flow, Macmillan, New York, USA.

Hicks, F. E., Steffler, P. M., Gerard, R. 1991. Finite element modeling of surge propagation and an application to the Hay River. Canadian Journal of Civil Engineering, 19(3), 454-462.

Lai, C.-J., Liu, C. L., Lin, Y.-Z. 2000. Experiments on flood-wave propagation in compound channel. Journal of Hydraulic Engineering - ASCE, 126(7), 492-501.

Lauber, G., Hager, W. H. 1998a. Experiments to dambreak wave: Horizontal channel. Journal of Hydraulic Research - IAHR, 36(3), 291-307.

Lauber, G., Hager, W. H. 1998b. Experiments to dambreak wave: Sloping channel. Journal of Hydraulic Research - IAHR, 36(5), 761-773.

Leal, J. G. A. B., Ferreira, R. M. L., Cardoso, A. H. 2006. Dam-break Wave Front Celerity. Journal of Hydraulic Engineering - ASCE, 132(1), 69-76.

Meile, T. 2007. Influence of macro-roughness of walls on steady and unsteady flow in a channel. Dissertation N° 3952 de l'Ecole Polytechnique Fédérale de Lausanne and Communication 36 of the Laboratory of Hydraulic Constructions (LCH-EPFL), Ed. A. Schleiss; ISSN 1661-1179.

Meile, T., Boillat, J.-L.; Schleiss, A., 2008a. Einfluss von großmaßstäblichen Uferrauheiten und Buchten auf Schwallwellen in Flüssen infolge Kraftwerksbetrieb. Wasser, energie, luft 100 (1), 6-12.

Meile, T.; Boillat, J.-L.; Schleiss, A. J. 2008b. Dämpfende Wirkung von grossmassstäblichen Uferrauheiten auf Schwall und Sunkerscheinungen in Flüssen. WasserWirtschaft 98 (12), 18-24.

Meile, T.; Boillat, J.-L.; Schleiss, A. J. 2008c. Improvement of Acoustic Doppler Velocimetry in steady and unsteady turbulent open-channel flows by means of seeding with hydrogen bubbles. Flow Measurement and Instrumentation, 19(3/4), 215-221; DOI:10.1016/j.flowmeasinst. 2007.08.009.

Morris, H. M. 1955. Flow in Rough Conduits. Transact. of the American Society of Civil Engineers, 120, 373-410.

Ponce, V. M., Li, R. M., Simons, D. B. 1978. Applicability of kinematic and diffusive models. Journal of Hydraulic Division - ASCE, 104(3), 353-360.

Rouse, H. 1965. Critical Analysis of Open-Channel Resistance. Journal of Hydraulics Division, 91(HY4), 1-25.
Schoklitsch, A. 1917. Ueber Dammbruchwellen. Sitzungsberichte der Kaiserlichen Akademie der Wissenschaften in Wien, 126(10), 1489-1514.
Sieben, J. 2003. Estimation of effective hydraulic roughness in non-uniform flow. XXX IAHR Congress, Thessaloniki, Greece, 17-24.
Soares-Frazao, S., Zech, Y. 2002. Undular bores and secondary waves - Experiments and hybrid finite - volume modelling. Journal of Hydraulic Research - IAHR, 40(1), 33-43.
Treske, A. 1994. Undular Bores (Favre-Waves) in Open Channels - Experimental Studies. Journal of Hydraulic Research - IAHR, 32(3), 355-370.
Uensal, I. 1983. Propagation of dam-break waves in channels of varying section. XX IAHR Congress, Moscow, U.S.S.R., 539-545.
Whitham, G. B. 1955. The effects of hydraulic resistance in the dam-break problem. Proceedings of the Royal Society A, 227, 399-407.
Zairov, K. I., Listrovoy, P. P. 1983. Experimental investigation of the positive traveling surges fore-part observed in canals. XX IAHR Congress, Moscow, U.S.S.R., 210-218.